



Platform development for high-throughput optimization of perfusion processes: Part I: Implementation of cell bleeds in microwell plates

Marie Dorn¹  | Kerensa Klottrup-Rees² | Ken Lee³ | Martina Micheletti¹ 

¹Department of Biochemical Engineering, Advanced Centre for Biochemical Engineering, University College London, London, UK

²Cell Culture and Fermentation Sciences, Biopharmaceutical Development, AstraZeneca, Cambridge, UK

³BioProcess Technologies and Engineering, Biopharmaceutical Development, AstraZeneca, Gaithersburg, Maryland, USA

Correspondence

Martina Micheletti, Advanced Centre for Biochemical Engineering, University College London, Bernard Katz Bldg, Gower St, London WC1E 6BT, UK.
Email: m.micheletti@ucl.ac.uk

Funding information

AstraZeneca; Engineering and Physical Sciences Research Council

Abstract

The promise of continuous processing to increase yields and improve product quality of biopharmaceuticals while decreasing the manufacturing footprint is transformative. Developing and optimizing perfusion operations requires screening various parameters, which is expensive and time-consuming when using benchtop bioreactors. Scale-down models (SDMs) are the most feasible option for high-throughput data generation and condition screening. However, new SDMs mimicking perfusion are required, enabling experiments to be run in parallel. In this study, a method using microwell plates (MWP) operating in semi-perfusion mode with an implemented cell bleed step is presented. A CHO cell line was cultivated in a 24-well MWP ($V_w = 1.2$ mL) and grown at four high cell density (HCD) setpoints. Quasi steady-state condition was obtained by manually performing cell bleeds followed by a total medium exchange after centrifugation. Further, two HCD setpoints were scaled up ($V_w = 30$ mL), comparing a squared six-well deepwell plate (DWP) to shake flasks (SF). This evaluation showed comparable results between systems (DWP vs. SF) and scales (MWP vs. DWP + SF). The results show that the well-plate-based methods are suitable to perform HCD and quasi steady-state cultivations providing a robust solution to industrially relevant challenges such as cell clone and media selection.

KEYWORDS

deepwell plate, high-throughput, microwell plate, perfusion, process development, small-scale

1 | INTRODUCTION

In recent years, the rising demand of biopharmaceuticals such as monoclonal antibodies (mAb) prompted the biopharmaceutical industry to push for next generation manufacturing strategies. The

development of end-to-end integrated continuous biomanufacturing will enable the industry to cover the demand and meet other challenges (e.g., product quality requirements, growing competition from biosimilars) (Arnold et al., 2019; Schwarz et al., 2022; Warikoo et al., 2012).

Abbreviations: Amm, ammonium; CHO, Chinese hamster ovary; CSPR, cell-specific perfusion rate; DWP, deepwell plate; Glc, glucose; Glu, glutamate; HCD, high cell density; HIP, high intensity perfusion medium; Lac, lactate; mAb, monoclonal antibody; MWP, microwell plate; RV, reactor volume; SDM, scale-down model; SF, shake flask; ST, spin tube; STY, space-time-yield; VCC, viable cell concentration.

This is an open access article under the terms of the [Creative Commons Attribution](https://creativecommons.org/licenses/by/4.0/) License, which permits use, distribution and reproduction in any medium, provided the original work is properly cited.

© 2024 The Authors. *Biotechnology and Bioengineering* published by Wiley Periodicals LLC.

Compared to the traditionally used fed-batch mode of operations, using a perfusion mode for cell cultivation and production has resulted in significantly increased volumetric productivities with values around $2 \text{ g L}^{-1} \text{ d}^{-1}$ (Xu et al., 2017). Most recently volumetric productivities of $>5 \text{ g L}^{-1} \text{ d}^{-1}$ have been reported (Wong et al., 2021). This increase is due to the combination of two main factors. First, the continuous medium exchange removes the supernatant, while replacing it with fresh medium, thus providing a stable environment within the cell culture (Chotteau, 2015). Second, cells are retained in the bioreactor using a cell retention device (e.g., alternating tangential flow filtration, ATF) which enables to achieve high cell densities (HCD) up to $120 \times 10^6 \text{ cells mL}^{-1}$ (Clincke, Mölleryd, Samani, et al., 2013; Clincke, Mölleryd, Zhang, et al., 2013). In most cases, cells are grown to a target density and then stably maintained at this “steady-state” cell concentration. This can be done by using either cell bleeds (Coolbaugh et al., 2021; Schwarz et al., 2022; Warikoo et al., 2012) or cell arrest approaches (Ahn et al., 2008; Ducommun et al., 2002).

Although, perfusion mode requires a lower capital and operational cost investment than fed-batch (Mahal et al., 2021), their design is complex due to the number of parameters to optimize. Developing and optimizing a perfusion bioreactor process requires screening multiple experimental conditions, which can be costly and time-consuming if done at laboratory scale (Wolf et al., 2018). Scale-down models (SDM), having working volumes in the milliliter or microliter scale, are the most feasible option to overcome this obstacle by collecting bioprocess information early on (Sao Pedro et al., 2021). For SDMs to be useful in this capacity, they are required to mimic the typical characteristics of a perfusion bioreactor, such as the medium exchange used within a perfusion system, and must be able to achieve as well as maintain HCD through cell retention and cell bleed at a “steady-state.” In addition to the operational features, a SDM should allow for high-throughput operation to run multiple conditions in parallel to be time-efficient during process development.

Previous studies investigated the automated mini bioreactor system ambr15 ($V_w = 10\text{--}15 \text{ mL}$) and showed its ability to mimic a perfusion process with perfusion rates up to 2 RV d^{-1} , where cell retention was achieved via sedimentation (Jin et al., 2021; Kreye et al., 2019; Sewell et al., 2019). Further, comparability to larger scale perfusion bioreactors was shown (Goletz et al., 2016; Kreye et al., 2019). Other studies investigated spin tubes (STs, $V_w = 10 \text{ mL}$) as an SDM in semi-perfusion, showing reliable representation of various process parameters like flow rates, productivities, and metabolite consumption rates (Bielser et al., 2019; Mayrhofer et al., 2021; Wolf et al., 2018). In these studies discontinued daily medium exchanges (known as semi-perfusion), and cell retention through centrifugation were used, and viable cell concentrations (VCC) up to $60 \times 10^6 \text{ cells mL}^{-1}$ could be achieved (Bielser et al., 2019). However, by using uncontrolled SDMs like ST, oxygen supply becomes the most critical parameter for HCD operations as aeration is provided through the free surface from the headspace. Studies have shown that low filling volumes and high agitation speeds support high volumetric gas transfer coefficients ranging from 20 to 110 h^{-1} sufficient to enable HCD (Zhu et al., 2017). However, STs are

not amenable to automation and would therefore not meet the demand for high-throughput experimentation and less labor-intensive protocols.

Recent studies have investigated 24-well microwell plates (MWP, $V_w = 1.2 \text{ mL}$) in semi-perfusion using a sacrificial well methodology as a small-scale platform for optimization of perfusion processes (Tregidgo et al., 2023). Similar to spin tubes, oxygen supply becomes critical at HCD for MWP formats. However, several studies evaluating a number of well geometries, shaking speeds, and fill volumes showed that sufficiently high $k_L a$ values can be reached to support HCD cultivations (Doig et al., 2005; Hermann et al., 2003; Zhang et al., 2008). For 24-well MWPs, maximum VCC values up to $60 \times 10^6 \text{ cells mL}^{-1}$ were reported, as well as good agreement with a 5 L bioreactor in perfusion mode (Tregidgo et al., 2023). In addition, MWPs can be automated more easily than STs or shake flasks (SF), allowing screening of several hundred conditions in parallel (Mayr & Bojanic, 2009; Silva et al., 2022), and can be integrated with associated analytics within the same robotic platform (Lambiase et al., 2022).

Nonetheless, a detailed understanding about the limitations and capabilities of MWP is still to be developed. Questions remain regarding the ability to mimic basic perfusion characteristics such as establishing and maintaining a stable environment. It was previously shown that HCD can be achieved in 24-well MWP (Tregidgo et al., 2023), and this study evaluates the platform regarding its capabilities of maintaining HCD at a specific target VCC and thus establishing a quasi-steady state at small scale. In this work this previously established semi-perfusion MWP method was adapted by implementing a cell bleed strategy into the workflow. This cell removal step aims at operating at approximately constant average VCC values (target VCC). In addition to MWP experimentation, a scale-up into a six-well deepwell plate (DWP) and SF, both operating at a working volume of 30 mL, was performed. The scale-up from MWP to SF comes with a change of geometry and operating conditions which result in different mixing patterns (i.e., aeration profiles) and potentially influence the cellular and process performance. The DWPs offer a scale-up alternative operating at similar scale as SF, while the handling of the culture is more equivalent to MWPs and could be easily automated. It is noteworthy that the respective geometries of MWP and DWP have some differences, as shown in the schematic diagram of each system presented in Figure 1a,b. For comparison to SDMs in literature, the geometry of spin tubes is shown as well (cf. Figure 1c). To compare the impact of geometry and handling during scale-up, DWP and SF cultivations were performed in parallel to investigate the influence on the cellular and process performance.

2 | MATERIALS AND METHODS

2.1 | Cell culture, cell line, and media

A Chinese hamster ovary (CHO) cell line, known as CHO cobra (Cobra Biologics AB) and producing the recombinant monoclonal antibody trastuzumab, was used for all experiments. Cells were cultivated in a

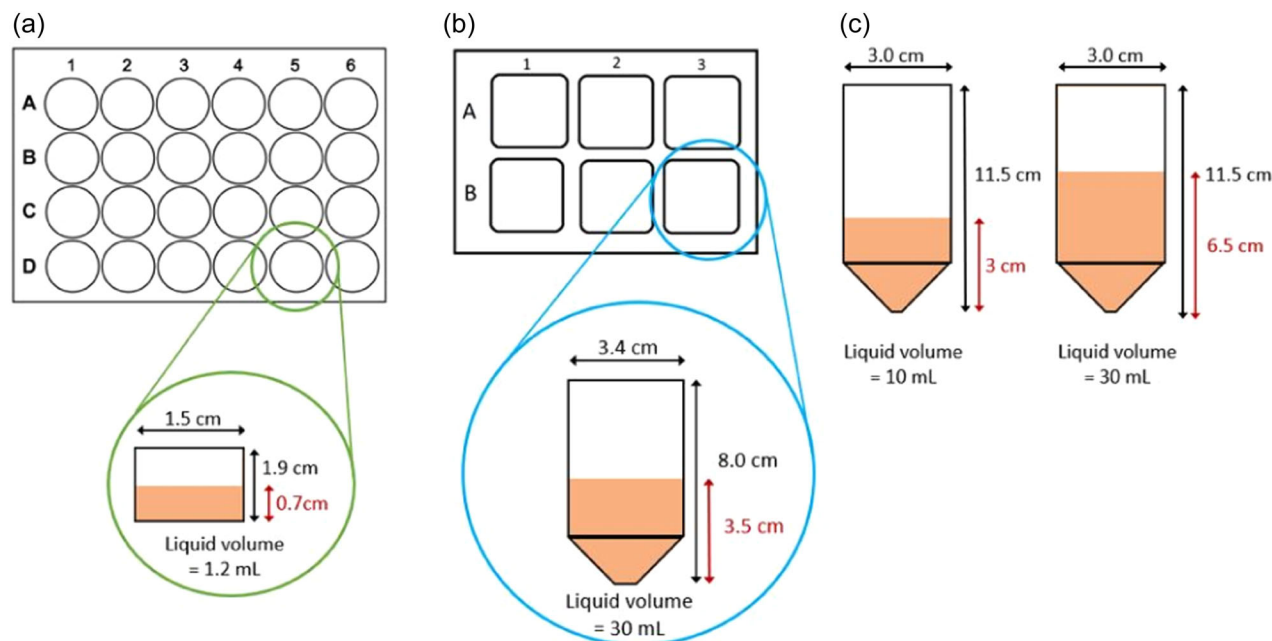


FIGURE 1 Schematic representation of three scale-down models (a) 24-standard round well microwell plate and single well dimensions; (b) squared six-well deepwell plate and single well dimension; and (c) spin tubes with two different working volumes.

perfusion-specific base medium named high intensity perfusion (HIP) medium (Gibco®; Thermo Fisher Scientific) supplemented with 3.2 mM GlutaMax™-I (100X) (Gibco®; Thermo Fisher Scientific) and 2% 1X HT supplement (Gibco®; Thermo Fisher Scientific). During experimentation, the base medium was blended with 30% CHO-CD EfficientFeed™ B (v/v) (Gibco®; Thermo Fisher Scientific), referred to as Feed B.

Cell suspensions were cultivated in 125 mL non-baffled SF (Corning®) placed in a CO₂ incubator (MCO-19AIC; Sanyo) at 37°C with 5% CO₂, and were agitated at a shaking speed of 180 rpm, using an orbital shaker (CO₂ resistant shaker; Thermo Fisher Scientific) with an orbital diameter (OD) of 25 mm. Cells were passaged every 3–4 days and expanded into 2 L SF (Corning®) used for inoculation. Two different precultures were used originating from the same working cell bank, one for MWP cultures and one for DWP/SF cultures.

2.2 | Process operations

2.2.1 | MWP cultures

MWP cultures were performed using standard round well ultra-low attachment 24-well MWP (CLS3473; Corning®) and operated using a sacrificial well methodology as previously described by Tregidgo et al. (2023). The plates were sealed with a Duetz sandwich lid (CR1524; EnzyScreen) to reduce evaporation while maintaining headspace gas exchange. All cultures were cultivated in a CO₂ incubator at 37°C, 5% CO₂, an agitation speed of 250 rpm, and an OD of 25 mm, if not otherwise indicated. The plates were held in place by a Duetz MWP clamp system (CR1801h; EnzyScreen).

The MWPs were inoculated at a seeding density close to the VCC target value at a working volume of 1.2 mL (day 0, cf. Figure 1). Samples were taken every 24 h in triplicates using a sacrificial well methodology, resulting in a cultivation duration of 8 days. In a first step, the VCC of three wells, so called “sampling wells,” was measured. Based on the measured VCC a cell bleed volume was calculated (Equation 1). The respective bleed rate can be calculated using Equation (2).

$$V_B = \frac{(X_m - X_{SP}) \times V_W}{X_m} \quad (1)$$

$$B = \frac{V_B}{V_W \times \Delta t} \quad (2)$$

Where V_B is the bleed volume, X_m the average of three measured VCC, X_{SP} the targeted setpoint VCC, V_W the working volume, B the bleed rate, and Δt the time interval between two sampling time points. The bleed volume was removed from the “culture wells” to reset the VCC in the culture. It is noteworthy that the VCC setpoint value for calculation was lower than the targeted VCC value required to maintain a stable average VCC. After cell bleeding, the MWPs were centrifuged at 50g for 5 min, followed by supernatant collection of the designated “sampling wells” for quantification of metabolites and titers. Subsequently, remaining supernatant in the “culture wells” was removed (total medium exchange) mimicking a perfusion rate of 1 RV d⁻¹. The complete workflow is shown in Figure 2.

The experimental runs targeted average VCCs of 10, 20, 30, and 40 × 10⁶ cells mL⁻¹ at 1 RV d⁻¹. The corresponding VCC setpoints were 8, 16, 24, and 32 × 10⁶ cells mL⁻¹, respectively.

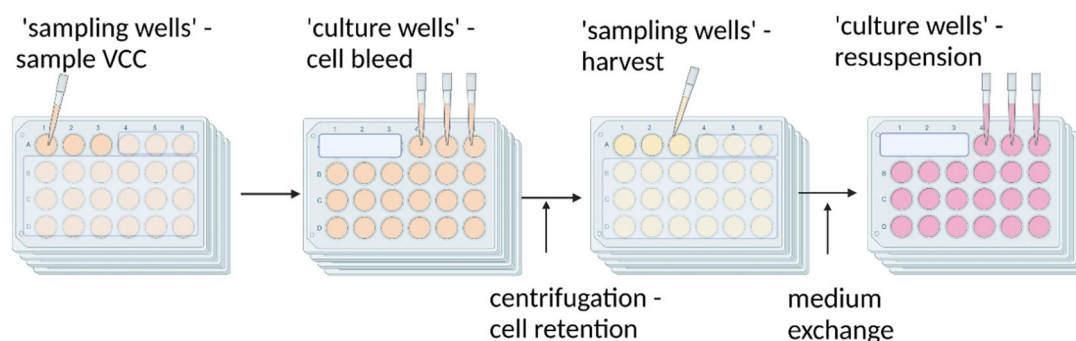


FIGURE 2 Schematic workflow of the sacrificial well methodology of MWP cultures in semi-perfusion. VCC is measured from samples taken from “sampling wells,” based on which a cell bleed to a VCC setpoint is performed for the remaining “culture wells.” After centrifugation, the “sampling wells” are emptied and the cell-free supernatant is collected for titer and metabolite quantification, while for the remaining “culture wells” a total medium removal is performed. Cells in “culture wells” are resuspended in fresh medium, and plates are placed back in the incubator. The workflow is repeated every 24 h over the course of 8 days, where the “sampling wells” and “culture wells” shift to the next three wells. Created with biorender.com. MWP, microwell plate; VCC, viable cell concentrations.

2.3 | DWP and SF cultures

DWP cultures were performed using squared six-well DWPs (CR1406; EnzyScreen). The plates were sealed with a Duetz sandwich lid (CR1206a; EnzyScreen) to reduce evaporation while maintaining headspace gas exchange. SF cultures were performed as triplicates using unbaffled 125 mL SF (polycarbonate Erlenmeyer culture flask Corning®). All cultures were cultivated and sampled using the same protocol as for the MWPs and performed over a duration of 10 days, where the day of inoculation marks day 0, if not otherwise indicated. VCCs were measured and used to calculate the bleed volume for each well and flask for DWP and SF, respectively. Due to the larger volume of DWP and SF, the amount taken for VCC measurements was considered negligible. Hence for the entire cultivation period the same three wells or SFs per condition were used. All cultures were placed in a CO₂ incubator at 37°C and 5% CO₂. DWPs were agitated at a speed of 250 rpm, an OD of 25 mm as suggested by the company and held in place by a Duetz MWP clamp system (CR1801h; EnzyScreen). SFs were agitated at a speed of 180 rpm and an OD of 25 mm, similar to the seed cultures. The DWPs and SF were inoculated close to the VCC targets with a working volume of 30 mL (day 0, Figure 1b,c). Samples were taken every 24 h in triplicates and centrifugation was performed at 50g for 10 min.

2.4 | Process analytics

VCC and percentage of viability were determined using a ViCell™ XR cell viability analyzer (Beckman Coulter). Due to the small sample size for MWP cultures, the number of extracellular metabolites was limited to 3, based on feedback from industry these were set to glucose, lactate, and ammonium. These were determined using an Optocell CuBiAn VC biochemistry analyzer

(4BioCell). Extracellular metabolites of DWP and SF cultures were determined with BioProfile FLEX analyzer (Nova Biomedical), where in addition to glucose, lactate, and ammonium, glutamate was determined. Both machines were previously validated using the same batch of medium and give comparable results (e.g., glucose concentration: 76.93 mmol L⁻¹ and 73.16 mmol L⁻¹). To determine mAb titers, a HPLC (HPLC Agilent 1100 series; Agilent) with 1 mL Protein G column (HiTrap™ Protein G HP; Cytiva) was used with a loading buffer A (20 mM phosphate, pH 7.0) and an elution buffer B (20 mM glycine, pH 2.8) to evaluate the protein concentration. An IgG standard with a concentration of 1.9 g L⁻¹ was used (determined by Nanodrop 1000; Labtech). The standard was diluted in PBS and measured in triplicate to obtain a standard curve between 0 and 1.9 g L⁻¹.

For the comparative analysis between different cultivation systems used, the cell-specific consumption and production rates of glucose, lactate, ammonium as well as mAb were calculated as daily average using the following equation.

$$q = \left(\frac{\Delta c}{\Delta t \times \bar{X}} \right) + \frac{(H + B) \times c_i}{\bar{X}} \quad (3)$$

Where q is the cell-specific consumption/production rate, H is the daily harvest rate, B is the daily bleed rate, Δt is the time interval between two sampling time points, \bar{X} is the daily average of the VCC, and c is the metabolite/product concentration.

3 | RESULTS

3.1 | Cultivation in MWPs

First, we investigated the cell bleed workflow in MWPs using a perfusion-specific base medium referred to as HIP. Previous studies investigating the same cell line and base medium found that an additional blend with 30% Feed B was optimal to support

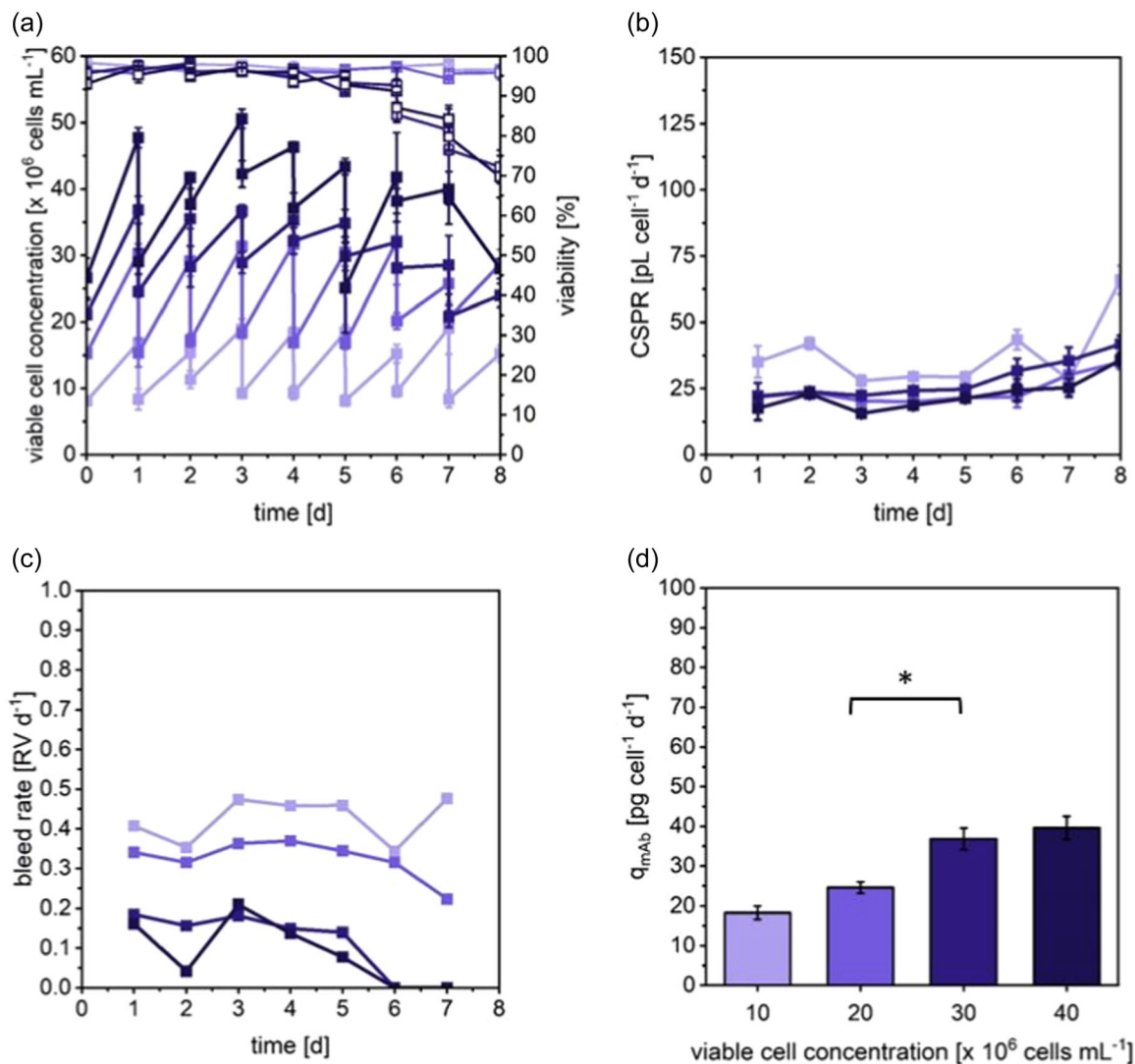


FIGURE 3 Viable cell concentrations, cell-specific perfusion rates, and bleed rates for CHO cells in 24-well MWP cultivations in semi-perfusion with implemented cell bleeds. Cells were inoculated at 10, 20, 30, and 40 $\times 10^6$ cells mL^{-1} and cultivated in HIP medium supplemented with 30% Feed B (v/v). (a) Growth (filled) and viability (open); (b) CSPR; (c) bleed rate; (d) cell-specific productivity (q_{mAb}). Targeted average VCCs ($\times 10^6$ cells mL^{-1}): 10 (■, light), 20 (■, medium-light), 30 (■, medium-dark), 40 (■, dark). Mean of $N = 3$ wells. Error bars indicate standard deviation. A t -test analysis was used to evaluate significant difference for conditions distinguished best-performing between VCC targets ($^*p < 0.05$). CHO, Chinese hamster ovary; HIP, high intensity perfusion medium; MWP, microwell plate; VCC, viable cell concentrations.

maximum growth to HCD and to achieve high productivities. Hence the HIP medium was blended with Feed B to support the maintenance of HCD targets.

Overall, four VCC target points (10, 20, 30, and 40 $\times 10^6$ cells mL^{-1}) were investigated. Figure 3 shows growth profiles, characteristic process, and production rates for cultivations in MWPs. For all four VCC setpoints a typical “saw-wave” growth profile could be maintained throughout the experiment’s duration (cf. Figure 3a). With the exception of conditions targeting setpoints of 30 and 40 $\times 10^6$ cells mL^{-1} , where growth was reduced and targeted VCCs were not reached at the end of the cultivation (day 8). Generally, growth was stable over the entire duration of the culture. This is supported by the largely stable bleed rate obtained for all conditions (cf. Figure 3c). For cultures

targeting a VCC setpoint of 10 $\times 10^6$ cells mL^{-1} , the bleed rate amounted to nearly 50% of the working volume, whereas a higher VCC setpoint resulted in a reduction of the bleed rate to 10%–20% of the working volume.

The CSPR was observed over time showing a stabilization after day 2 for all conditions. Depending on the targeted VCC the CSPR stabilized at different levels, where lower CSPRs were established for higher VCC targets. For all conditions, CSPRs rose steadily towards the end of the cultivation, with larger increases observed for the VCC setpoint of 10 $\times 10^6$ cells mL^{-1} on day 8.

Surprisingly, the cell-specific productivities increased with increasing VCC targets, where the highest q_{mAb} observed was 39.6 ± 2.8 pg cell $^{-1}$ d $^{-1}$ for the VCC target 40 $\times 10^6$ cells mL^{-1} (cf. Figure 3d). Between the setpoint of 20 and 30 $\times 10^6$ cells mL^{-1}

differences of approximately 5% were observed. Significant differences between other setpoints were not evaluated as only the VCC setpoints of 20 and 30×10^6 cells mL^{-1} were subsequently investigated in further detail (cf. Sections 3.2 and 3.3). A total medium exchange was performed after the bleed and centrifugation step (c.f. Section 2.3), where each condition received fresh media from the same origin to reduce the impact of slightly different media compositions on the q_{mAb} .

Due to the limited working volume, the number of metabolites measured was limited to glucose, lactate, and ammonium. These were chosen as the typically monitored and controlled metabolites in industry. Similar to CSPR and bleed rate observations, the metabolite concentrations of lactate and glucose stabilized after day 1 and 2, respectively (cf. Figure 4a,b). Although glucose concentrations showed larger fluctuation over time, a general trend was observable, where for high VCC targets

the average glucose concentrations were the lowest (14.2 mmol L^{-1} for a VCC target of 40×10^6 cells mL^{-1}). Lactate concentrations showed only minor fluctuations but counterintuitive results, where conditions targeting the lowest VCC setpoint obtained the highest lactate concentrations. For example, for the VCC target of 10×10^6 cells mL^{-1} , a lactate concentration of 15.5 mmol L^{-1} was obtained, while the corresponding glucose concentration was also the highest at 42.8 mmol L^{-1} . It is known that cells convert glucose into lactate with an approximate ratio of 1:2, where one mole glucose is converted in two mole lactate. Hence, it was expected to see high lactate concentrations for cultivations with low glucose concentrations, that is, conditions targeting higher VCC setpoints. A hypothesis was a shift in metabolism from lactate production to consumption for high VCC setpoints (30 and 40×10^6 cells mL^{-1}), which was further assessed by calculating the lactate to glucose yield ($Y_{\text{Lac/Glc}}$). A metabolism shift would be

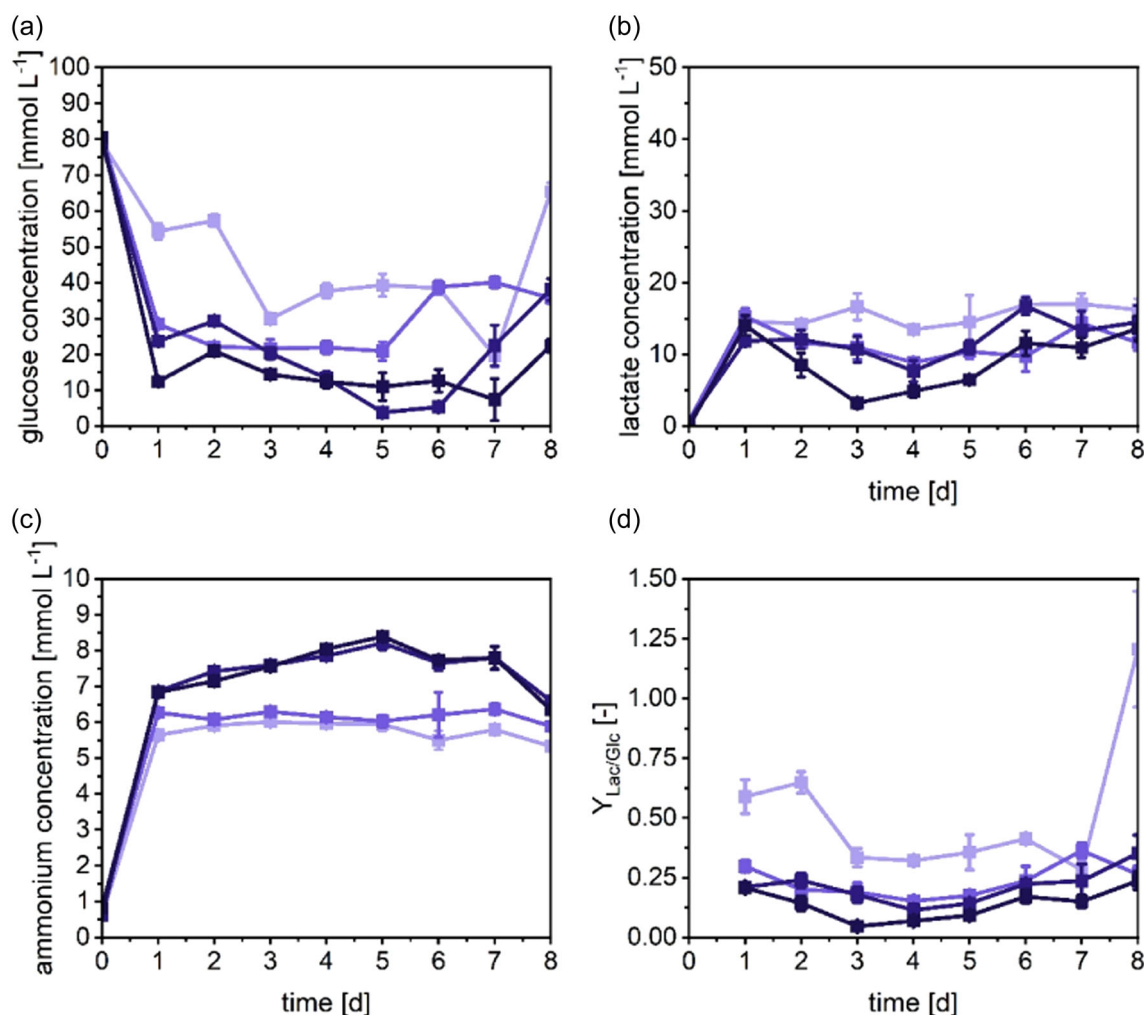


FIGURE 4 Metabolite concentrations for CHO cells in 24-well microwell plate cultivations in semi-perfusion with implemented cell bleeds. Cells were inoculated at 10, 20, 30, and 40×10^6 cells mL^{-1} and cultivated in HIP medium supplemented with 30% Feed B (v/v). (a) Glucose concentration; (b) lactate concentration; (c) ammonium concentration; (d) $Y_{\text{Lac/Glc}}$. Targeted average VCCs ($\times 10^6$ cells mL^{-1}): 10 (■, light), 20 (■, medium-light), 30 (■, medium-dark), 40 (■, dark). Mean of $N = 3$ wells. Error bars indicate standard deviation. CHO, Chinese hamster ovary; HIP, high intensity perfusion medium; VCC, viable cell concentrations.

indicated by a decrease of $Y_{\text{Lac/Glc}}$. However, the constant trend, with a slight increase from day 4 onwards, suggested a stable conversion of glucose to lactate. Further, it showed that for the lowest VCC setpoint of 10×10^6 cells mL^{-1} the $Y_{\text{Lac/Glc}}$ values were two-fold higher than for all other setpoints (cf. Figure 4d). Ammonium concentrations remained stable between 5.5 and 8.5 mmol L^{-1} throughout the cultivation. Interestingly, the concentrations obtained stabilized at two distinct levels, at around 6 mmol L^{-1} for VCC setpoints of 10 and 20×10^6 cells mL^{-1} and at around 7.5 mmol L^{-1} for the setpoints of 30 and 40×10^6 cells mL^{-1} (cf. Figure 4c). It was expected to see four different stabilization levels similar to what was observed for other metabolites evaluated.

3.2 | Cultivations in SFs and DWPs

Following the investigation of the MWP, the two best performing conditions were transferred from a MWP scale into larger scale typical for SF cultivations ($V_w = 30$ mL). Best performing conditions were distinguished as a trade-off between stable cell growth, metabolic state and productivity to be the VCC targets of 20 and 30×10^6 cells mL^{-1} . In this work, a novel DWP setup was investigated in parallel to SF cultures and evaluated based on cellular performance and manual handling. Hence, results obtained were evaluated at the same scale (DWP vs. SF) as well as across scales (MWP vs. DWP + SF). The agitation speed of DWP cultures was the same as previously used for MWP, further the supplier suggested an optimal range of 225 rpm at OD of 25 mm for CHO cell cultures. As the experiments target HCD cultures the increase to 250 rpm, the same speed as MWP, allows for better comparability as well as ensures good oxygen transfer. SF cultures were agitated at 180 rpm for safety concerns. In opposite to the plates, which is supported by a clamp system securing the plates tightly in the incubator, SF are standing without further clamping support on the shaker table. Concerns about oxygen limitation due to the slower agitation speed were evaluated, however the larger gas-liquid surface area and no visible drop in viability in previous lab-internal studies at higher cell concentration (data not shown) led to the conclusion that the operating conditions are sufficient to support the targeted VCC.

All cultivations show the previously seen “saw-wave” VCC profile, which could be maintained over the entire process duration of 10 days (cf. Figure 5a). Similar to MWP cultures, the DWP condition targeting a VCC of 30×10^6 cells mL^{-1} showed a growth reduction on the last 2 days of culture (cf. Figures 5a and 3a). This corresponds to a reduction in the viability to 80%–90%, observed from day 5, and further reduction below 70% on day 10. In contrast to the DWP cultures, all conditions in SFs largely maintained viabilities above 95% throughout the culture duration. Analogous to MWP cultures, the CSPRs stabilized after day 2 at around 30 and 40 $\text{pL cell}^{-1} \text{d}^{-1}$ for the VCC targets 20 and 30×10^6 cell mL^{-1} , respectively. These levels were maintained with a slight increase at the end of the cultivation (cf. Figure 5b). The bleed rate stabilized at two different

levels depending on the VCC targeted, whereby the bleed rates were largely similar between the cultivation systems (cf. Figure 5c). For the conditions with the lower VCC target of 20×10^6 cells mL^{-1} the bleed rate of around 0.3 RV d^{-1} was higher compared to 0.1 RV d^{-1} for the higher VCC target. The same trend was previously observed for the MWP cultivation experiments.

Cell-specific mAb production rates (q_{mAb}) were comparable at 20 and 30×10^6 cells mL^{-1} for DWP cultivations, with no significant difference. Comparing both cultivation systems, a significant difference at the 5% level ($p < 0.05$) was found at the VCC target of 20×10^6 cells mL^{-1} , but no significant difference was found for the higher VCC target. Productivities of around 30 $\text{pg cell}^{-1} \text{d}^{-1}$ could be achieved with both systems at the larger VCC target of 30×10^6 cells mL^{-1} (cf. Figure 5d).

The evaluation of metabolites for both setpoints and cultivation systems showed similar dynamics with a stabilization of glucose and lactate concentrations following the start of semi-perfusion (cf. Figure 6a,b). Ammonium concentrations were stable throughout the cultivation with concentrations below 10 mmol L^{-1} with average values between 5.3 and 8.0 mmol L^{-1} with a slight increase at the end of culture (data not shown). However, due to larger sample volumes available for the DWP and SF cultivations, an additional parameter could be measured, where extracellular glutamate concentrations showed surprising results (cf. Figure 6c,d). For cultures in DWPs targeting 30×10^6 cells mL^{-1} , the specific glutamate production rate was significantly larger ($p < 0.05$) than for other cultures. The glutamate concentration increased starting on day 4 which corresponds with the observed reduced viability in this culture following day 5 (cf. Figure 6c). Since the DWP cultivation targeting 30×10^6 cells mL^{-1} showed a decrease in viability and higher glutamate concentrations this could potentially have influenced the cell-specific mAb production rate, resulting in nearly identical values at both VCC targets for the DWP compared to the increase observed for SF cultivations. For SF cultures, a significant difference ($p < 0.05$) between both setpoints was obtained with larger q_{Gluc} at 20×10^6 cells mL^{-1} . This could have influenced the cell-specific productivity which was observed to be significantly lower ($p < 0.01$) than for corresponding DWP cultures.

3.3 | Comparison across scales: MWP versus DWP and SF

To make a realistic comparison across scales, characteristic rates such as specific growth rate, bleed rate, and cell specific mAb production rates are presented in Figure 7, while cell specific glucose consumption, lactate, and ammonium production rates and lactate to glucose ratio ($Y_{\text{Lac/Glc}}$) are presented in Figure 8 and compared at the two VCC targets of 20 and 30×10^6 cells mL^{-1} .

Independent of the cultivations system used, the observed specific growth rates were similar at both VCC targets showing a decrease of their value with increasing VCC. Due to their direct dependence on cellular growth, the bleed rates decreased as well.

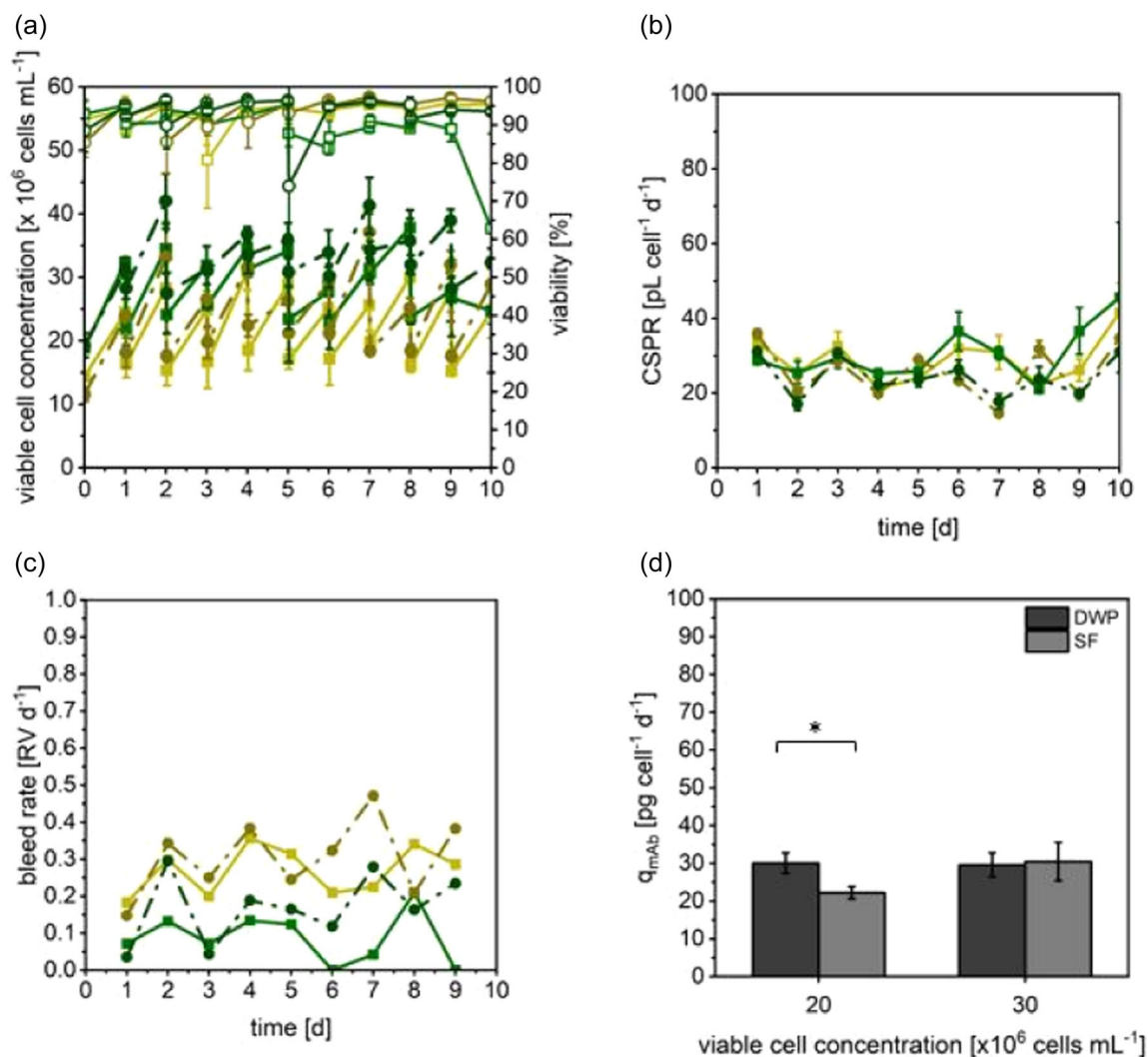


FIGURE 5 Viable cell concentrations, cell-specific perfusion rates, and bleed rates for CHO cells in six-well deepwell plate and shake flask (SF) cultivations in semi-perfusion with implemented cell bleeds. Cells were inoculated at 20 and 30 × 10⁶ cells mL⁻¹ and cultivated in high-intensity perfusion (HIP) medium supplemented with 30% Feed B (v/v). (a) Growth (filled) and viability (open); (b) CSPR; (c) bleed rate; (d) cell-specific productivity (q_{mAb}). SDM model: DWP (■, light), SF (●, dark), targeted average VCCs (×10⁶ cells mL⁻¹): 20 (yellow), 30 (green), mean of N = 3 wells. Error bars indicate standard deviation. (d) Cell-specific productivity. Significant difference was observed between cultivation systems and VCC targets (*p < 0.05). CHO, Chinese hamster ovary; DWP, deepwell plate; SDM, scale-down model; VCC, viable cell concentrations.

Specific growth rates decreased from 0.02 to 0.01 h⁻¹ and bleed rates from 0.3 to 0.1 RV d⁻¹. Although the cell bleed and total medium exchange to achieve a perfusion rate of 1 RV d⁻¹ was performed once a day for all three systems, it should be noted that procedures differed slightly between cultures in well plates (MWP, DWP) and SF. After removal of cells, SF cultures had to be transferred into centrifuge tubes before centrifugation. Following the centrifugation, the supernatant was removed, and the cells resuspended in fresh medium before transferring back into SFs. In contrast for MWP and DWP cell bleeds, centrifugation and medium exchange could be handled directly within the system.

Cell-specific mAb productivity was comparable over all culture systems and VCC targets. At 20 × 10⁶ cells mL⁻¹, a statistical

difference at a 5% level was found between DWP and MWP, but not at a 1% level as previously found between SF and DWP (cf. Figure 5d). Table 1 gives a comparison of titers and productivities achieved in MWPs, DWPs, and SFs as compared to studies using spin tubes as a SDM.

Cell-specific glucose consumption rates (q_{Glc}) are largely similar over the three cultivation systems without statistical significance (cf. Figure 8a). Similar results were obtained for cell-specific lactate (q_{Lac}) and ammonium (q_{Am}) production rates (cf. Figure 8b,c). Cell-specific lactate production rates in all cultivation systems at the setpoint of 20 × 10⁶ cells mL⁻¹ were slightly higher than at the VCC setpoint of setpoint of 30 × 10⁶ cells mL⁻¹. The lowest q_{Lac} was obtained for SF cultures at the higher setpoint but were within error range. However, no significant

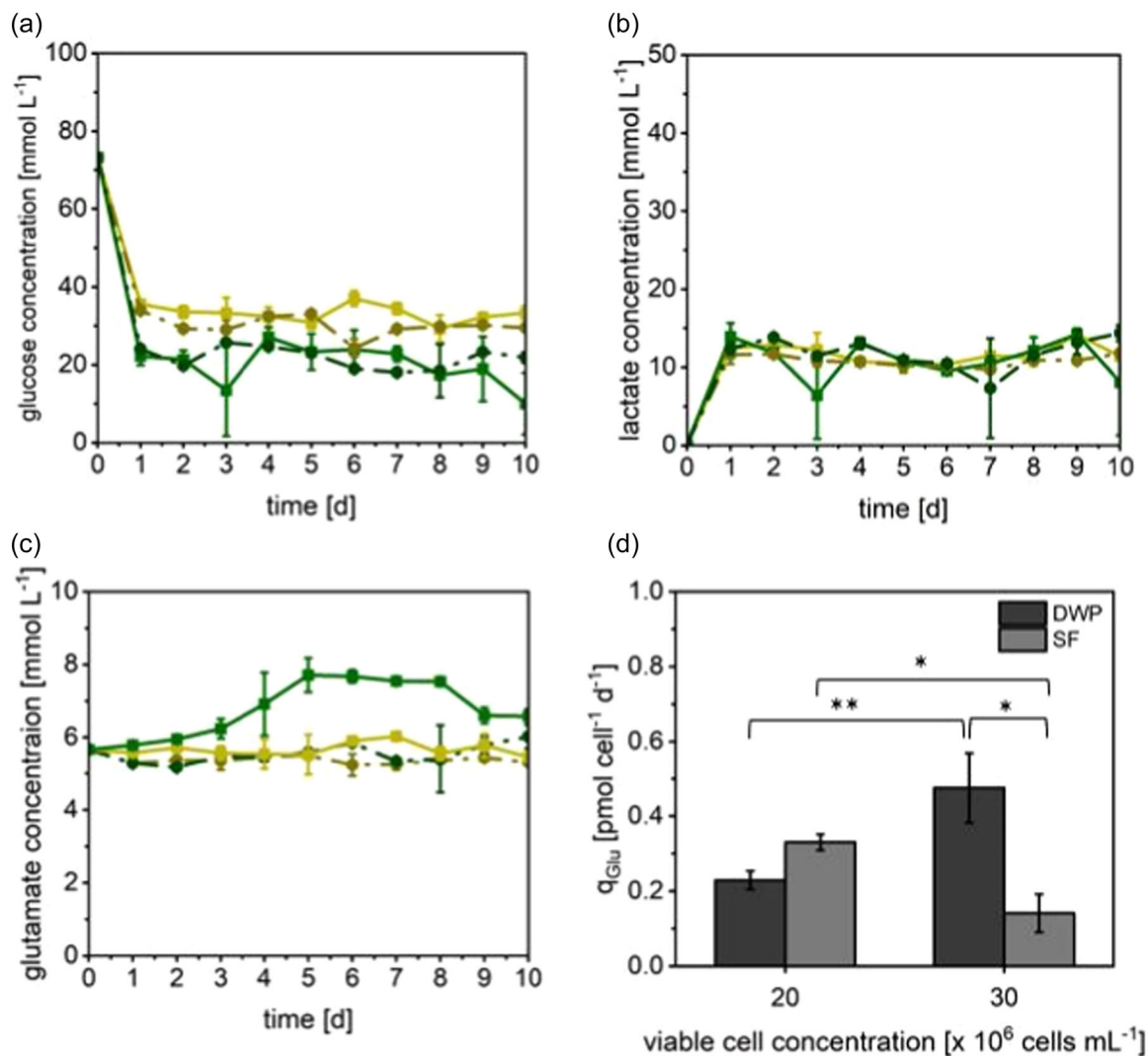


FIGURE 6 Metabolite concentrations for CHO cells in six-well deepwell plate and shake flask (SF) cultivations in semi-perfusion with implemented cell bleeds. Cells were inoculated at 20 and 30 × 10⁶ cells mL⁻¹ and cultivated in high-intensity perfusion (HIP) medium supplemented with 30% Feed B (v/v). (a) Glucose; (b) lactate; (c) glutamate, SDM model: DWP (■, light), SF (●, dark), targeted average VCCs (×10⁶ cells mL⁻¹): 20 (yellow), 30 (green). Mean of N = 3 wells. Error bars indicate standard deviation. (d) Cell-specific glutamate production rate. The larger working volume of DWP and SF cultivations provided enough material for an additional metabolite, glutamate, to be measured. A t-test analysis was used to evaluate significant difference for cell-specific glutamate production rate between cultivation systems and VCC targets (*p < 0.05, **p < 0.001). CHO, Chinese hamster ovary; DWP, deepwell plate; SDM, scale-down model; VCC, viable cell concentrations.

difference was observed. Similar results were obtained for q_{Amm} . Overall, q_{Lac} and q_{Amm} remained below 1.0 pmol cell⁻¹ d⁻¹ in all culture systems and for all VCC targets. In addition to the cell-specific consumption and perfusion rates, the lactate to glucose yield ($Y_{\text{Lac/Glc}}$) was calculated, shown in Figure 8d. It can be seen that for MWP cultures the values of $Y_{\text{Lac/Glc}}$ initially decreased to minimum values between 0.11 and 0.15 mmol_{Lac} mmol_{Glc}⁻¹ on day 4 before increasing till the end of cultivation on day 8. This is in contrast to DWP and SF cultures, where $Y_{\text{Lac/Glc}}$ was stable throughout. For both VCC targets, the values were in similar range in all cultivation systems.

It is worth mentioning that the screening of the two conditions in MWPs consumed around 260 mL medium using the sacrificial well

methodology over a duration of 8 days, whereas each larger scale system (DWP or SF) consumed about 1800 mL to investigate the same two conditions over a duration of 10 days using the same DWP or SF throughout. This equals a nearly sevenfold increase in medium consumption.

3.4 | Impact of medium supplementation on cellular growth and production performance

Lastly, in this work the impact of the Feed B supplementation on the growth and productivity in quasi steady-state growth cultures was investigated. As Feed B is known to improve growth, and

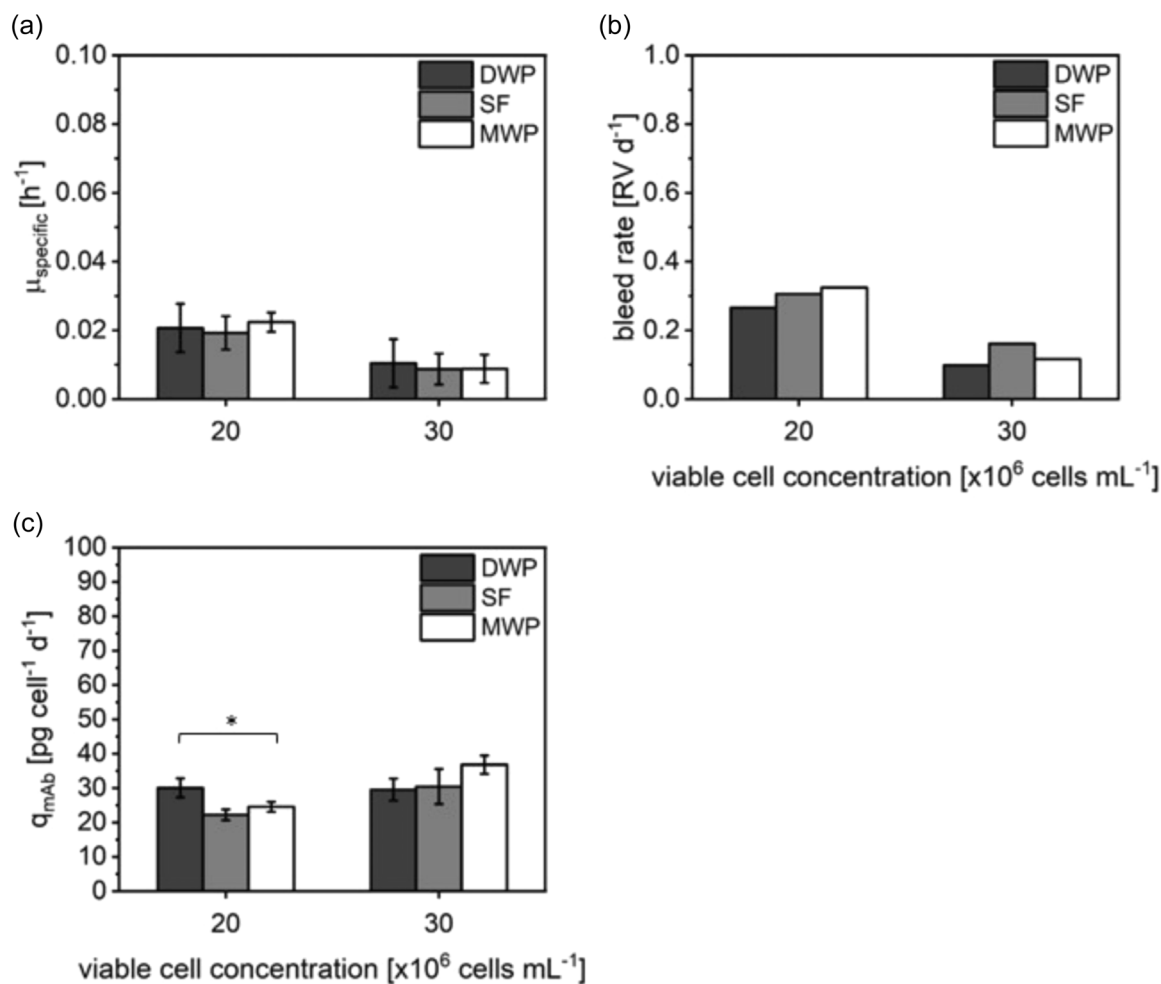


FIGURE 7 Comparison between values at steady state for MWP, DWP, and SF cultures. Cultures were inoculated at 20 and 30 $\times 10^6$ cells mL^{-1} and cultivated in high-intensity perfusion (HIP) medium supplemented with 30% Feed B. (a) Growth rate; (b) bleed rate; (c) cell specific mAb production (q_{mAb}). Mean of $N = 3$ wells. Error bars indicate standard deviation. A t -test analysis was used to evaluate significant difference between cultivation systems for mAb production ($*p < 0.05$). DWP, deepwell plate; mAb, monoclonal antibody; MWP, microwell plate; SF, shake flask.

thus mAb production, it was hypothesized that for quasi steady-state the influence of Feed B is marginal. To investigate this, additional experiments in MWPs were performed at the VCC setpoint of 10×10^6 cells mL^{-1} in HIP medium without Feed B supplementation.

To maintain stable growth at the low VCC target additional Feed B supplementation was found not to have an impact, as similar "saw-wave" profiles were obtained (cf. Figure 9a). For the cell-specific mAb production rates, a marginal increase could be observed for cultures with 30% Feed B supplementation. However, this difference was found to be not significant at a 5% level (not significant for $p < 0.05$). It is worth to note that a significant difference between both supplementations was found at a 7% level ($p < 0.07$) (cf. Figure 9b). This could be an indicator that positive effects of Feed B supplementation on growth and productivity are only present at higher VCC targets.

4 | DISCUSSION

In this study, we have investigated the feasibility of MWPs as a small-scale model ($V_w = 1.2$ mL) to operate at a quasi steady-state with cell bleeds. Further, a squared six-well DWP was evaluated against SF cultivations as this represents a novel option for scale-up to 30 mL working volume, using conditions previously performed in MWP experiments. The results were then compared across scales and cultivation systems.

The implementation of a cell bleed step aimed at establishing a quasi steady-state environment to the cell culture. The results show that by maintaining an average VCC, the CSPR and metabolite concentrations stabilized after day 2, suggesting an overall stable metabolism of the CHO cell culture resulting in stable bleed rates and mAb production throughout the cultivations for all conditions tested.

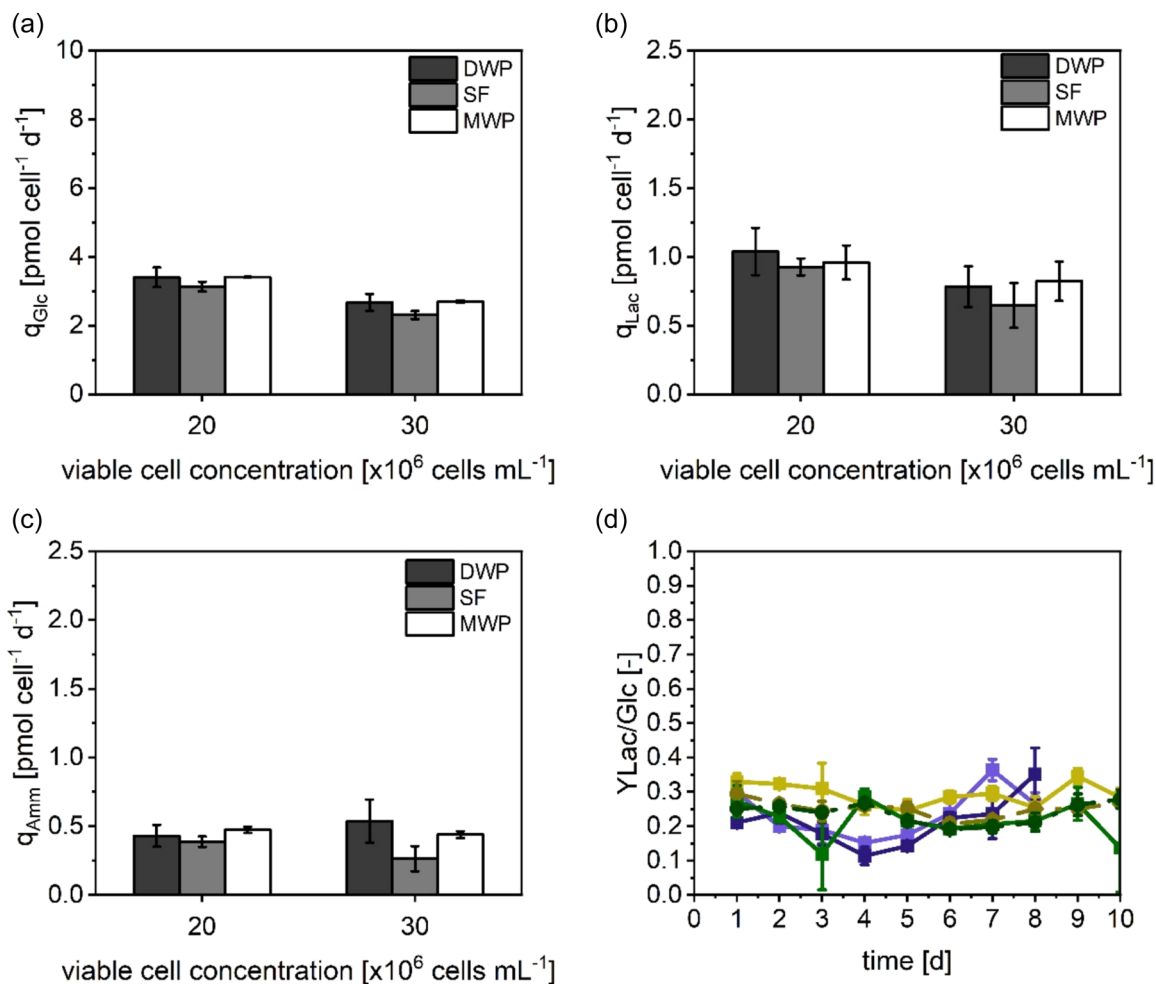


FIGURE 8 Comparison between values at steady state for MWP, DWP, and SF cultures. Cultures were inoculated at 20 and 30 × 10⁶ cells mL⁻¹ and cultivated in high-intensity perfusion (HIP) medium supplemented with 30% Feed B. (a) q_{Glc}; (b) q_{Lac}; (c) q_{Amm}; (d) Y_{Lac/Glc} yield. Mean of N = 3 wells. Error bars indicate standard deviation. MWP (■, violet), DWP (■, green), SF (●, yellow), targeted average VCCs (×10⁶ cells mL⁻¹): 20 (light), 30 (dark). Amm, ammonium; DWP, deepwell plate; Glc, glucose; Lac, lactate; MWP, microwell plate; SF, shake flask; VCC, viable cell concentrations.

Previous studies evaluated spin tubes ($V_w = 10$ mL) with a cell bleed strategy in semi-perfusion as a SDM to design and optimize bioreactor operations in a steady-state perfusion using suspension CHO cell line with chemically defined media (Mayrhofer et al., 2021; Wolf et al., 2018). It was shown that spin tubes give a reliable representation of a perfusion bioreactor for various process parameters (i.e., productivity, flow rates, steady-state stability) and it was argued that even better comparability can be achieved when using a more automated system (Wolf et al., 2018). However, spin tubes lack suitable capabilities for automation and thus remain labor intensive and limited in throughput. For MWP, automated systems are already established for fed-batch operations (Wang et al., 2018), while a suitable methodology able to mimic perfusion operations still needs to be thoroughly investigated.

In this work, a previously established workflow for MWPs in semi-perfusion was further adapted by implementing a cell bleed step. The results obtained in MWPs regarding key process parameters such as flow rates, growth, and productivities are improved to

previous studies investigating STs (Mayrhofer et al., 2021; Wolf et al., 2018), while similar observations were made for metabolite dynamics. Especially for lactate concentrations, we found higher lactate concentrations at low VCC targets in MWPs, similar to what was reported previously in STs (Wolf et al., 2018). This indicates that MWPs in semi-perfusion with cell bleed can be an equally suitable but alternative tool to predict certain parameter for steady-state perfusion bioreactors. Although the limited working volume of MWP provides challenges regarding the analysis of metabolites, key metabolites such as glucose and lactate (typically monitored in industry) as well as ammonium, were investigated to give initial insights on cellular process performance, which can inform in perfusion bioreactor cultivations. Nonetheless, MWPs have the advantage to be more easily automated than STs, hence providing the possibility for high-throughput investigations in a better controlled and monitored system.

In addition to the MWP, we investigated the novel DWP format as a new possibility when considering the scale-up to a V_w of 30 mL.

TABLE 1 Comparison of scale-down models in semi-perfusion with implemented cell bleed. Literature values are compared to experimental MWP, DWP, and SF results obtained for cultivations with perfusion medium in regards of productivities and perfusion parameters.

Reference/experiment	SDM	V_w [mL]	VCC target [$\times 10^6$ cells mL^{-1}]	mAb titer [g L^{-1}]	q_{mAb} [$\mu\text{g cell}^{-1} \text{d}^{-1}$]
Wolf et al. (2018), ^{ab}	ST	10	10	0.1 ± 0.01	N/A
			20	0.21 ± 0.01	10.12 ± 0.65
			30	0.32 ± 0.03	N/A
			40	N/A	10.00 ± 1.77
			30	N/A	N/A
Mayrhofer et al. (2021) ^c	ST	10	46	0.7	18
			45	0.6	16
Microwell culture in quasi steady-state condition ^d	MWP	1.2	10	0.11 ± 0.01	18.3 ± 1.6
			20	0.26 ± 0.01	24.5 ± 0.1
			30	0.49 ± 0.03	36.8 ± 2.6
			40	0.68 ± 0.03	39.6 ± 2.8
Scale-up of quasisteady-state condition ^e	DWP	30	20	0.33 ± 0.03	30.1 ± 2.7
			30	0.41 ± 0.05	29.57 ± 3.2
	SF		20	0.26 ± 0.01	22.2 ± 1.5
			30	0.49 ± 0.03	30.5 ± 5.1

Abbreviations: CHO, Chinese hamster ovary; DWP, deepwell plate; mAb, monoclonal antibodies; MWP, microwell plate; N/A, data not available; P, perfusion rate; q_{mAb} , cell-specific productivity; RV, reactor volume; SDM, scale down model; SF, shake flask; ST, spin tube; VCC, viable cell concentration; V_w , working volume.

^aValues are given for the last 5 days of culture; proprietary CHO cell line in chemically defined medium (both Merck).

^bProductivity and titer values were not measured due to reduced cellular performance caused by oxygen limitation.

^cValues are given for days 6–14 of culture; CHO-K1 cell line in ActiPro + CB1/3 or NS0 + CB1/3.

^dValues are given for 8 days of culture.

^eValues are given for 10 days of culture.

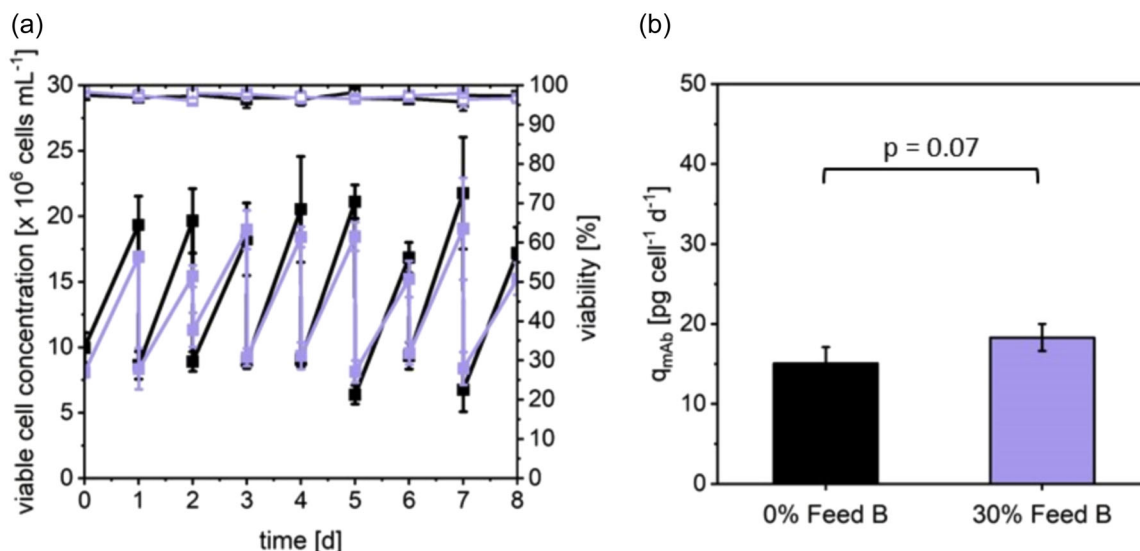


FIGURE 9 Growth and productivities for CHO cells in 24-well microwell plate cultivations in semi-perfusion with implemented cell bleeds. Cells were inoculated at 10×10^6 cells mL^{-1} and cultivated in base medium without Feed B (■, dark) or supplemented with 30% Feed B (v/v) (□, light). (a) Growth (filled) and viability (open). Mean of $N = 3$ wells. Error bars indicate standard deviation. (b) Cell-specific productivity. A significant difference was observed between base media and Feed B supplementation at $p = 0.07$. CHO, Chinese hamster ovary.

The geometry (liquid height, inner diameter and bottom shape, cf. Figure 1) of a single well of the DWP used in this study is more similar to a ST than to a SF. A previous study evaluated the influence of different working volume in STs comparing cultures with working volumes of 10 mL and 30 mL at 20 and 40×10^6 cells mL^{-1} (Wolf et al., 2018). The outcome of this study was that similar growth performance was observed at the lower VCC target in both working volumes. However, at the higher VCC, cellular growth could not be maintained in STs which was hypothesized to be caused by limited oxygen supply (Wolf et al., 2018). In the DWP format, growth was largely maintained throughout the process for both VCC targets, although a decrease of viability was observed at higher VCCs during and at the end of the cultivation. One hypothesis is that insufficient oxygen supply could have caused the viability reduction, however in the DWP format a decrease of viability was initially observed, and the cellular growth slowed down only at the end of the cultivation. It is noteworthy that the highest VCC target investigated in the DWP was 30×10^6 cells mL^{-1} , while the ST investigated a VCC of 40×10^6 cells mL^{-1} . It is possible that although the working volume is identical, the VCCs targeted are different and oxygen limitations could become problematic in the DWP format at even higher VCCs. Another hypothesis for the reduced viability (from day 5 onwards) observed in DWP cultures is that, although the lactate concentration was similar and stable for all conditions, the increase in extracellular glutamate concentration on top of the lactate concentration resulted in a reduction of pH. However, this hypothesis was only developed after the metabolite measurements were performed and cannot be verified as the pH value was not measured at the time of sampling. Additional studies are planned to further investigate this. Further, the focus for metabolite analysis in this study was set on toxic by-products as many industrial cell lines use a GS system enabling cell culture without addition of glutamine, which led to the analysis of glutamate instead of glutamine. Future investigations could include the analysis of nutrients such as glutamine as well for CHO cells requiring glutamine addition.

The comparison of DWP and SF cultivations showed that both systems obtained very similar results regarding growth and productivities with slight differences on average VCC, which were higher in SF cultures. This is most likely due to differences during the centrifugation step. While the centrifugation of MWP results in a tightly packed cell pellet where the medium removal can be performed without disturbing the pellet, the volume in DWP and SF is much larger, which requires either more time or higher speed or a combination of both for separation of cells and medium. SF cultures had to be transferred to 50 mL centrifuge tubes before centrifugation and were then centrifuged at a higher speed as published in literature (Bielser et al., 2019; Mayrhofer et al., 2021; Wolf et al., 2018), while the DWP was centrifuged as an entire system at the same speed as MWP cultures but for a prolonged time compared to MWP. This resulted in a less tightly packed cell pellet in the DWP compared to SF (as well as MWP) cultures and most likely a greater unintended loss of cells during medium removal. The centrifugation is an important step in the workflow and further investigation and

optimization is currently in progress. Nevertheless, the handling of the DWP was straightforward without the need for additional consumables (i.e., centrifuge tubes), whereas the SF cultures were more labor intensive, requiring the transfer of the culture into and out of 50 mL centrifuge tubes. The additional consumables needed would add to costs and display a risk for contamination during the transfers. Further, the investigation of two conditions in triplicates in the DWP format required less incubator space than the SF cultures as well as less consumables (1 DWP vs. 6 SF) which make the process more sustainable by using less energy and consumables. Both DWPs and SFs were able to replicate similar cell growth and productivity values reported for MWPs, thus showing comparability between scales and similarities to reported values in literature. However, in our opinion, the DWP system gave a slightly better representation of the MWP mainly because of two points. First, at the higher VCC target of 30×10^6 cells mL^{-1} , the growth reduced for the last 2 days in both DWP and MWP cultivations, but not in SFs. Second, at the VCC target of 20×10^6 cells mL^{-1} the q_{mAb} improved with the scale-up from MWP to DWP but decreased in the scale-up from MWP to SF. Given these similarities between MWP and DWP, a combined approach of MWP (small HT scale) and DWP (intermediate HT scale) could be suggested as a reliable and automatable SDM for a bioreactor.

5 | CONCLUSION

In this work, we showed the feasibility of MWPs to be operated in quasi steady-state semi-perfusion with cell bleeds at working volumes of 1.2 mL while maintaining VCCs of up to 40×10^6 cells mL^{-1} . In addition, we investigated the scale-up of conditions from the 24-well round MWP to a novel six-well squared DWP in comparison to the classic SF. Both platforms gave a good representation of the MWP cultures, however DWPs represented certain observations (i.e., growth) of the MWPs better. Showing the capabilities of both the MWP and DWP, we suggest to strategically combine these tools during process development. A possible case of application would be to use MWPs for condition screening targeting multiple set cell concentrations and possibly with multiple cell clones. In the next step, a selection of promising conditions could be transferred into DWPs which are similarly operated non-instrumented models with larger working volumes. This would provide more material for in-depth investigations of additional parameters such as metabolites and product quality, possibly allowing to further narrow down the chosen conditions before transferring a selected set of parameters into perfusion bioreactors at bench-scale to fine-tune the process.

AUTHOR CONTRIBUTIONS

Conceptualization: Marie Dorn and Martina Micheletti. *Methodology:* Marie Dorn. *Formal analysis:* Marie Dorn. *Investigation:* Marie Dorn. *Resources:* Martina Micheletti. *Data curation:* Marie Dorn. *Writing—original draft preparation:* Marie Dorn. *Writing—review and editing:* Marie Dorn, Martina Micheletti, Kerensa Klottrup-Rees,

and Ken Lee. *Visualization*: Marie Dorn. *Supervision*: Martina Micheletti, Kerensa Klottrup-Rees, and Ken Lee. *Project administration*: Martina Micheletti. *Funding acquisition*: Martina Micheletti. All authors have read and agreed to the published version of the manuscript.

ACKNOWLEDGMENTS

The author Marie Dorn would like to thank Ciara Lucas for constructive discussions and excellent technical support. Further, the author wants to thank Thomas Duetz and EnzyScreen for the provision of the six-well deepwell plate samples used in this study. The authors acknowledge Diane Hatton and Suzy Farid for their assistance in reviewing the manuscript. Financial support from the UK Engineering and Physical Sciences Research Council (EPSRC) and AstraZeneca for the Engineering Doctorate studentship for M. Dorn is gratefully acknowledged (Grant Ref: EP/S021868/1). This research is associated with the joint UCL-AstraZeneca Centre of Excellence for predictive decision-support tools in the bioprocessing sector and is aligned with the EPSRC Future Targeted Healthcare Manufacturing Hub hosted by UCL Biochemical Engineering.

CONFLICT OF INTEREST STATEMENT

The authors declare no conflict of interest.

DATA AVAILABILITY STATEMENT

The data that support the findings of this study are available from the corresponding author upon reasonable request.

ORCID

Marie Dorn  <http://orcid.org/0000-0002-5188-258X>

Martina Micheletti  <http://orcid.org/0000-0001-5147-0182>

REFERENCES

- Ahn, W. S., Jeon, J.-J., Jeong, Y.-R., Lee, S. J., & Yoon, S. K. (2008). Effect of culture temperature on erythropoietin production and glycosylation in a perfusion culture of recombinant CHO cells. *Biotechnology and Bioengineering*, 101(6), 1234–1244. <https://doi.org/10.1002/bit.22006>
- Arnold, L., Lee, K., Rucker-Pezzini, J., & Lee, J. H. (2019). Implementation of fully integrated continuous antibody processing: Effects on productivity and COGm. *Biotechnology Journal*, 14(2), e1800061. <https://doi.org/10.1002/biot.201800061>
- Bielser, J. M., Domaradzki, J., Souquet, J., Broly, H., & Morbidelli, M. (2019). Semi-continuous scale-down models for clone and operating parameter screening in perfusion bioreactors. *Biotechnology Progress*, 35(3), e2790. <https://doi.org/10.1002/btpr.2790>
- Chotteau, V. (2015). Perfusion processes. In M. Al-Rubeai (Ed.), *Animal Cell Culture* (Vol. 9, pp. 407–443). Springer.
- Clincke, M. F., Mölleryd, C., Samani, P. K., Lindskog, E., Fäldt, E., Walsh, K., & Chotteau, V. (2013). Very high density of Chinese hamster ovary cells in perfusion by alternating tangential flow or tangential flow filtration in WAVE Bioreactor-part II: Applications for antibody production and cryopreservation. *Biotechnology Progress*, 29(3), 768–777. <https://doi.org/10.1002/btpr.1703>
- Clincke, M. F., Mölleryd, C., Zhang, Y., Lindskog, E., Walsh, K., & Chotteau, V. (2013). Very high density of CHO cells in perfusion by ATF or TFF in WAVE bioreactor. Part I. Effect of the cell density on the process. *Biotechnology Progress*, 29(3), 754–767. <https://doi.org/10.1002/btpr.1704>
- Coolbaugh, M. J., Varner, C. T., Vetter, T. A., Davenport, E. K., Bouchard, B., Fiadeiro, M., Tugcu, N., Walther, J., Patil, R., & Brower, K. (2021). Pilot-scale demonstration of an end-to-end integrated and continuous biomanufacturing process. *Biotechnology and Bioengineering*, 118(9), 3287–3301. <https://doi.org/10.1002/bit.27670>
- Doig, S. D., Pickering, S. C. R., Lye, G. J., & Baganz, F. (2005). Modelling surface aeration rates in shaken microtitre plates using dimensionless groups. *Chemical Engineering Science*, 60(10), 2741–2750. <https://doi.org/10.1016/j.ces.2004.12.025>
- Ducommun, P., Ruffieux, P. A., Kadouri, A., Von Stockar, U., & Marison, I. W. (2002). Monitoring of temperature effects on animal cell metabolism in a packed bed process. *Biotechnology and Bioengineering*, 77(7), 838–842. <https://doi.org/10.1002/bit.10185>
- Goletz, S., Stahn, R., & Kreye, S. (2016). Small scale cultivation method for suspension cells.
- Hermann, R., Lehmann, M., & Büchs, J. (2003). Characterization of gas-liquid mass transfer phenomena in microtiter plates. *Biotechnology and Bioengineering*, 81(2), 178–186. <https://doi.org/10.1002/bit.10456>
- Jin, L., Wang, Z. S., Cao, Y., Sun, R. Q., Zhou, H., & Cao, R. Y. (2021). Establishment and optimization of a high-throughput mimic perfusion model in ambr[®] 15. *Biotechnology Letters*, 43(2), 423–433. <https://doi.org/10.1007/s10529-020-03026-5>
- Kreye, S., Stahn, R., Nawrath, K., Goralczyk, V., Zoro, B., & Goletz, S. (2019). A novel scale-down mimic of perfusion cell culture using sedimentation in an automated microbioreactor (SAM). *Biotechnology Progress*, 35(5), e2832. <https://doi.org/10.1002/btpr.2832>
- Lambiase, G., Inman, S. E., Muroi, M., Lindo, V., Dickman, M. J., & James, D. C. (2022). High-throughput multiplex analysis of mAb aggregates and charge variants by automated two-dimensional size exclusion-cation exchange chromatography coupled to mass spectrometry. *Journal of Chromatography A*, 1670, 462944. <https://doi.org/10.1016/j.chroma.2022.462944>
- Mahal, H., Branton, H., & Farid, S. S. (2021). End-to-end continuous bioprocessing: Impact on facility design, cost of goods, and cost of development for monoclonal antibodies. *Biotechnology and Bioengineering*, 118(9), 3468–3485. <https://doi.org/10.1002/bit.27774>
- Mayr, L. M., & Bojanic, D. (2009). Novel trends in high-throughput screening. *Current Opinion in Pharmacology*, 9(5), 580–588. <https://doi.org/10.1016/j.coph.2009.08.004>
- Mayrhofer, P., Castan, A., & Kunert, R. (2021). Shake tube perfusion cell cultures are suitable tools for the prediction of limiting substrate, CSPR, bleeding strategy, growth and productivity behavior. *Journal of Chemical Technology & Biotechnology*, 96(10), 2930–2939. <https://doi.org/10.1002/jctb.6848>
- São Pedro, M. N., Silva, T. C., Patil, R., & Ottens, M. (2021). White paper on high-throughput process development for integrated continuous biomanufacturing. *Biotechnology and Bioengineering*, 118(9), 3275–3286. <https://doi.org/10.1002/bit.27757>
- Schwarz, H., Gomis-Fons, J., Isaksson, M., Scheffel, J., Andersson, N., Andersson, A., Castan, A., Solbrand, A., Hober, S., Nilsson, B., & Chotteau, V. (2022). Integrated continuous biomanufacturing on pilot scale for acid-sensitive monoclonal antibodies. *Biotechnology and Bioengineering*, 119(8), 2152–2166. <https://doi.org/10.1002/bit.28120>
- Sewell, D. J., Turner, R., Field, R., Holmes, W., Pradhan, R., Spencer, C., Oliver, S. G., Slater, N. K., & Dikicioglu, D. (2019). Enhancing the functionality of a microscale bioreactor system as an industrial process development tool for mammalian perfusion culture. *Biotechnology and Bioengineering*, 116(6), 1315–1325. <https://doi.org/10.1002/bit.26946>

- Silva, T. C., Eppink, M., & Ottens, M. (2022). Automation and miniaturization: Enabling tools for fast, high-throughput process development in integrated continuous biomanufacturing. *Journal of Chemical Technology & Biotechnology*, 97(9), 2365–2375. <https://doi.org/10.1002/jctb.6792>
- Tregidgo, M., Lucas, C., Dorn, M., & Micheletti, M. (2023). Development of mL-scale pseudo-perfusion methodologies for high-throughput early phase development studies. *Biochemical Engineering Journal*, 195, 108906. <https://doi.org/10.1016/j.bej.2023.108906>
- Wang, B., Albanetti, T., Miro-Quesada, G., Flack, L., Li, L., Klover, J., Burson, K., Evans, K., Ivory, W., Bowen, M., Schoner, R., & Hawley-Nelson, P. (2018). High-throughput screening of antibody-expressing CHO clones using an automated shaken deep-well system. *Biotechnology Progress*, 34(6), 1460–1471. <https://doi.org/10.1002/btpr.2721>
- Warikoo, V., Godawat, R., Brower, K., Jain, S., Cummings, D., Simons, E., Johnson, T., Walther, J., Yu, M., Wright, B., McLarty, J., Karey, K. P., Hwang, C., Zhou, W., Riske, F., & Konstantinov, K. (2012). Integrated continuous production of recombinant therapeutic proteins. *Biotechnology and Bioengineering*, 109(12), 3018–3029. <https://doi.org/10.1002/bit.24584>
- Wolf, M. K. F., Lorenz, V., Karst, D. J., Souquet, J., Broly, H., & Morbidelli, M. (2018). Development of a shake tube-based scale-down model for perfusion cultures. *Biotechnology and Bioengineering*, 115(11), 2703–2713. <https://doi.org/10.1002/bit.26804>
- Wong, H. E., Chen, C., Le, H., & Goudar, C. T. (2021). From chemostats to high-density perfusion: The progression of continuous mammalian cell cultivation. *Journal of Chemical Technology & Biotechnology*, 97(9), 2297–2304. <https://doi.org/10.1002/jctb.6841>
- Xu, S., Gavin, J., Jiang, R., & Chen, H. (2017). Bioreactor productivity and media cost comparison for different intensified cell culture processes. *Biotechnology Progress*, 33(4), 867–878. <https://doi.org/10.1002/btpr.2415>
- Zhang, H., Lamping, S. R., Pickering, S. C. R., Lye, G. J., & Shamlou, P. A. (2008). Engineering characterisation of a single well from 24-well and 96-well microtitre plates. *Biochemical Engineering Journal*, 40(1), 138–149. <https://doi.org/10.1016/j.bej.2007.12.005>
- Zhu, L., Song, B., Wang, Z., Monteil, D. T., Shen, X., Hacker, D. L., De Jesus, M., & Wurm, F. M. (2017). Studies on fluid dynamics of the flow field and gas transfer in orbitally shaken tubes. *Biotechnology Progress*, 33(1), 192–200. <https://doi.org/10.1002/btpr.2375>

How to cite this article: Dorn, M., Klottrup-Rees, K., Lee, K., & Micheletti, M. (2024). Platform development for high-throughput optimization of perfusion processes: Part I: Implementation of cell bleeds in microwell plates. *Biotechnology and Bioengineering*, 1–15. <https://doi.org/10.1002/bit.28682>